

Supporting Information

Stolk et al. 10.1073/pnas.1414886111

SI Materials and Methods

Behavioral Data Analysis. We considered mean planning times (Fig. S1 *B* and *C*), mean movement times, and mean number of moves of Communicator and Addressee within the fMRI session. These dependent variables were calculated for each of the 27 pairs of participants and for each of the two problem types (Known, Novel), and compared statistically by means of paired *t* tests (two-tailed α level = 0.05). We considered the pairs of participants as the unit of observation for the statistical analysis of task performance, as communicative success is dependent of both elements of a pair. The pairs spent on average 20.1 ± 0.3 s within each communicative interaction (mean interaction length \pm SEM) and jointly solved the interactions well above chance level ($71 \pm 2\%$ correct, mean \pm SEM; conservative estimate of chance level: one-eighth, eight potential goal locations, neglecting the potential orientations). They solved more Known ($94 \pm 1\%$, mean \pm SEM) than Novel interactions ($47 \pm 4\%$); $t_{(26)} = 13.6$, $P < 0.001$ (Fig. S1*D*). In a similar vein, the participants planned longer [Communicators: $t_{(26)} = 5.9$, $P < 0.001$; Addressees: $t_{(26)} = 8.5$, $P < 0.001$; Fig. S1 *B* and *C*], moved longer [Communicators: $t_{(26)} = 8.1$, $P < 0.001$; Addressees: $t_{(26)} = 13.2$, $P < 0.001$], and made more moves [Communicators: $t_{(26)} = 3.1$, $P < 0.005$; Addressees: $t_{(26)} = 17.7$, $P < 0.001$] within the Novel interactions than within the Known interactions. These findings indicate that the Known interactions were easier than the Novel interactions, most likely because of the different types of goal configurations faced by the participant pairs within these interactions, and because these interactions were completed before during the training session outside the scanners (*Materials and Methods, Experimental Design*). However, the focus of this study is not on these trivial differences in difficulty, but rather on the change in communicative success during Novel interactions over the course of the experiment (a marker for the emergence of meaning within pairs). We selected between a linear and a logarithmic function to describe this change, with the latter providing a better fit [$F_{(1,40)} = 51.6$, $P < 0.001$, $R^2_{\text{adj}} = 0.55$; green curve in Fig. S1*D*] than the former [$F_{(1,40)} = 35.2$, $P < 0.001$, $R^2_{\text{adj}} = 0.46$]. Accordingly, we used a logarithmic function to parameterize time-related changes in BOLD signal within Novel and Known interactions (see *Materials and Methods, fMRI image acquisition and analysis*).

Previous work showed stronger coupling between Communicator and Addressee planning times than between players of a noncommunicative control interaction (1). This observation suggests that the new communicative problems encountered by the participants evoked stronger mutual adjustments between pairs than the noncommunicative problems. Here, we performed a similar cross-correlation analysis, separately for planning times of Communicators and Addressees evoked during Known and Novel interactions. In the Novel interactions, the within-interaction coupling between Communicator and Addressee planning times was stronger within real communicative pairs ($r = 0.15 \pm 0.18$, mean \pm SD) than within random pairs [$r = 0.06 \pm 0.16$; $t_{(727)} = 2.8$; $P = 0.006$, two-sided independent *t* test]. There was no such significant difference on the Known interactions (real pairs: $r = 0.09 \pm 0.17$; random pairs: $r = 0.06 \pm 0.17$). This observation suggests that a Novel communicative problem was concomitantly more difficult for both Communicators and Addressees of the same pair, emphasizing the shared load of the communicative challenge across both elements of a pair.

Communication Strategies. Within the communication game, the pairs have to develop particular strategies to convey a message about the goal configuration of the Addressee's token. To understand how communication was established despite the limited means available in this game, we performed a qualitative analysis describing pairs' behaviors evoked during the Novel trials. In contrast to the Known trials, the problem types of the Novel trials were not presented to the pair before (*Materials and Methods, Experimental Design*), offering the possibility to qualify how participants establish shared meanings of the behaviors in the task. To achieve a balance between identifying an interpretable (i.e., limited) number of communicative strategies and describing each and every trial in each pair of participants, we considered seven categories:

- i) Pause strategy (occurrence: 17%). The Communicator marks the Addressee's goal location by spending more time at the goal location compared with other visited locations of the game board.
- ii) Wiggle strategy (41%). The Communicator moves away from the Addressee's goal location to one of its adjacent locations on the board (in the direction the Addressee's token should point), and back again to the Addressee's goal location. We also observed Communicators to repeat this action (e.g., [Movie S1](#)).
- iii) Center-out strategy (7.6%). The Communicator moves away from the center of the game board (at movement onset) along the direction the Addressee's token should point, before moving toward the Addressee's goal location (and using strategy *i* to mark that location). We also observed Communicators to return to the center of the game board, having indicated the Addressee's goal orientation, before moving toward the Addressee's goal location (e.g., [Movie S2](#)).
- iv) Target-out strategy (9.6%). The Communicator moves away from the Addressee's goal location along the direction the Addressee's token should point, before moving to his own goal location. We also observed Communicators to exaggerate this target-out movement, moving their token along the whole row or column of the Addressee's goal position (e.g., [Movie S3](#)).
- v) Rotation-matching strategy (10%). The Communicator rotates his token at the Addressee's goal location as many times the Addressee needs to rotate. This strategy only worked if the Communicator controlled a token other than a circular token, as the rotations of a circular token are not visible to either player.
- vi) Rotation-drawing strategy (1.9%). The Communicator mimics the desired rotational movements of the Addressee by drawing circles on the game board (e.g., [Movie S4](#)).
- vii) Other (12.9%). For some trials, the strategy could not be identified or its occurrence was too infrequent to deserve a category on its own.

Different strategies could be used at the same time. For instance, Communicators frequently distinguished the Addressees' goal locations from other visited locations on the game board by using a short pause (strategy *i*) at the respective location, independently from an additional strategy to indicate Addressee's goal orientations (e.g., a "wiggle"). Although pausing alone seems insufficient for indicating goal configurations that involve a specific orientation, we also observed pairs to use the pausing strategy in situations where previously used strategies to indicate

a goal orientation did not suffice. For instance, we observed that a pair had converged on a wiggling strategy to indicate goal orientations, but when the players are presented with a goal configuration involving a triangle that points “outward” (i.e., wiggling along the axis the triangle should point is no longer an option), they converged on using the pausing strategy (i.e., the absence of a wiggle) for this complex goal configuration. Interestingly, the exact same behavior had a quite different meaning in earlier trials of the same pair (see movie S4 A–D of ref. 1), indicating how the meanings of behaviors in this game depend on the current conversational context of a pair.

Fig. S2 illustrates representative communicative dynamics across three communicative pairs over the course of the Novel interactions. In the “spiderplot,” the spokes represent individual trials, increasing in clockwise direction. The rings represent the different communication strategies used across the group. It can be seen that pairs neither use a single stereotyped strategy, neither continuously explore a wide range of possible strategies. This observation makes a clear case for the notion that, in this game, the selection of communicative behaviors depends on the shared communicative history of a pair. More precisely, it can be seen that, within each pair, there is considerable variation across strategies in the first trials of the communicative task. This indicates that Communicators do not rely on a strategy that they think is “correct,” and then leave Addressees to figure out what that strategy might be. Different pairs do not necessarily converge on the same strategy, a further indication that there is no correct or privileged way of solving this communicative task. Furthermore, when pairs converge on the meaning of a communicative behavior, they may appeal to this shared meaning in later trials. For instance, participant pair 19 (black line in Fig. S2) converges on strategy *iv* at trial 10 and frequently uses the same strategy in later trials.

Control Analyses. Several control analyses were performed to test for alternative interpretations of the findings obtained with coherence spectral-density analysis. First, it could be argued that interpersonal cerebral coherence in right superior temporal gyrus (rSTG) (Fig. 2C) is driven by coherent changes in attention to the auditory stimulation of the MR scanners. Accordingly, we performed a coherence analysis on rSTG BOLD signal time series after removal of cortical signals related to auditory stimulation, as indexed by time series of BOLD signal obtained from the primary auditory cortex (ref. 2; see Fig. S6A for voxelwise functional connectivity maps of activity that was regressed out before computing coherence). The pair-specific low-frequency interpersonal coherence in the rSTG remained statistically significant (with maximum coherence at 0.0125 Hz, $P = 0.016$; Fig. S6B). Second, it could be argued that the interpersonal coherence observed in the rSTG is driven by coherent changes in visual attention and eye movement. Accordingly, we performed a coherence analysis on rSTG BOLD signal time series after removal of cortical signals related to eye movement, as indexed by time series of BOLD signal obtained from the frontal eye fields (ref. 3; see Fig. S7A for voxelwise functional connectivity maps of activity that was regressed out before computing coherence). The

pair-specific low-frequency interpersonal coherence in the rSTG remained statistically significant (with maximum coherence at 0.0375 Hz, $P = 0.002$; Fig. S7B). Third, it could be argued that the interpersonal coherence observed in the rSTG is driven by coherent task-induced modulations of brain activity within the default-mode network (4). Accordingly, we performed a coherence analysis on rSTG BOLD signal time series after removing default-mode activity, as indexed by time series of BOLD signal from the posterior cingulate cortex (ref. 4; see Fig. S8A for voxelwise functional connectivity maps). The pair-specific low-frequency interpersonal coherence in the rSTG remained statistically significant (with maximum coherence at 0.0125 Hz, $P = 0.004$; Fig. S8B). Furthermore, the shared cerebral dynamics could not be accounted for by participants’ confusion about their communicative roles, because those roles were fixed across the experiment. Fourth, we tested whether the interpersonal coherence in the rSTG, despite the fact that its frequency spanned several communicative interactions, might have been driven by trial-specific features. Accordingly, we performed a coherence analysis on BOLD signal time series in which trial-specific features were removed through multiple regression. This was accomplished by constructing a multiple-regression model that considered all seven task epochs (Fig. S1A), with planning epochs of Communicators, observation epochs of Addressees, and feedback epochs modeled separately for each problem type (Known, Novel) and outcome (Positive, Negative). This model considered a total of nine regressors for each Communicator and Addressee, respectively. The interpersonal coherence analysis was performed on the residuals of that multiple-regression analysis. The pair-specific low-frequency interpersonal coherence in the rSTG remained statistically significant, with stronger coherence in real pairs than in random pairs (with maximum coherence at 0.035 Hz, $P = 0.006$; Fig. S9B). In contrast, the pair-specific interpersonal coherence at the dominant experimental frequency observed in the left sensorimotor cortex (Fig. 2H) was severely affected by this control analysis (Fig. S9C and D). More precisely, coherence at the dominant experimental frequency disappeared, although higher frequency harmonic components still survived (Fig. S9D). This finding emphasizes that interpersonal coherence in rSTG, unlike left sensorimotor cortex, was driven by abstract features independent from trial-specific elements of the communicative interactions. Fifth, we tested whether the pair-specific and state-specific cerebral synchronization between participants’ BOLD signals was specific to the rSTG (Fig. 2E). Accordingly, we performed coherence spectral-density analyses and pair/state-specific synchronization analyses on a number of cortical regions previously suggested to be involved in social action understanding and perspective taking (5–8). Neither left inferior frontal gyrus (6), right inferior parietal lobule (7), right temporoparietal junction (5), or ventromedial prefrontal cortex (8) showed interpersonal coherence effects that were influenced by the emergence of mutual understanding (Fig. S10). Those sites lacked the pair-specific and state-specific response profile observed in the rSTG.

1. Stolk A, et al. (2013) Neural mechanisms of communicative innovation. *Proc Natl Acad Sci USA* 110(36):14574–14579.
2. Bandettini PA, Jesmanowicz A, Van Kylen J, Birn RM, Hyde JS (1998) Functional MRI of brain activation induced by scanner acoustic noise. *Magn Reson Med* 39(3):410–416.
3. Cheng K, Fujita H, Kanno I, Miura S, Tanaka K (1995) Human cortical regions activated by wide-field visual motion: An H2(15)O PET study. *J Neurophysiol* 74(1):413–427.
4. Raichle ME, et al. (2001) A default mode of brain function. *Proc Natl Acad Sci USA* 98(2):676–682.
5. Young L, Camprodon JA, Hauser M, Pascual-Leone A, Saxe R (2010) Disruption of the right temporoparietal junction with transcranial magnetic stimulation reduces the role of beliefs in moral judgments. *Proc Natl Acad Sci USA* 107(15):6753–6758.
6. Kilner JM, Neal A, Weiskopf N, Friston KJ, Frith CD (2009) Evidence of mirror neurons in human inferior frontal gyrus. *J Neurosci* 29(32):10153–10159.
7. Chong TT, Cunnington R, Williams MA, Kanwisher N, Mattingley JB (2008) fMRI adaptation reveals mirror neurons in human inferior parietal cortex. *Curr Biol* 18(20):1576–1580.
8. Lewis PA, Rezaie R, Brown R, Roberts N, Dunbar RI (2011) Ventromedial prefrontal volume predicts understanding of others and social network size. *Neuroimage* 57(4):1624–1629.

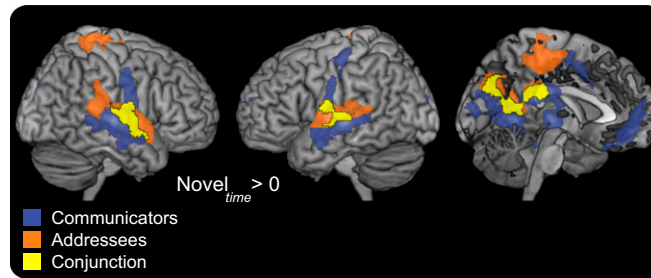


Fig. 54. Main effect of time—imaging results. Brain regions showing a logarithmic increase in BOLD signal over the course of the experiment during Novel problem types, during production (in Communicators) and comprehension of communicative signals (in Addressees). The statistical maps are thresholded at $P < 0.05$, whole-brain FWE corrected; see Table S1 for details. As expected on basis of the behavioral data, there were no significant changes in cerebral activity over the course of the Known interactions that yielded overlapping activity patterns between the two roles.

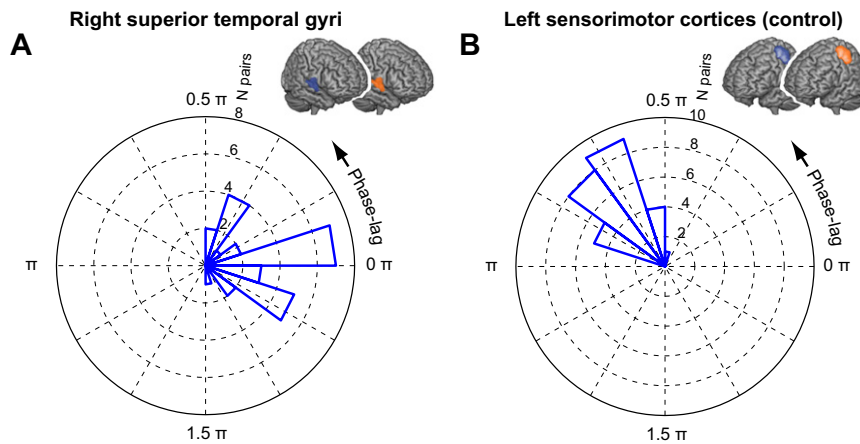


Fig. 55. Phase-lag of cerebral dynamics of Communicators and Addressees. The angle histograms show phase-lag estimates across the group, corresponding to cerebral coherence within the 0.01- to 0.04-Hz frequency range of rSTG dynamics (A) and cerebral coherence at 0.05 Hz of left sensorimotor cortex dynamics (B). The spokes of the angle histograms represent phase-lags, increasing in anticlockwise direction. The rings represent the number of participant pairs with phase-lags falling within an identical bin.

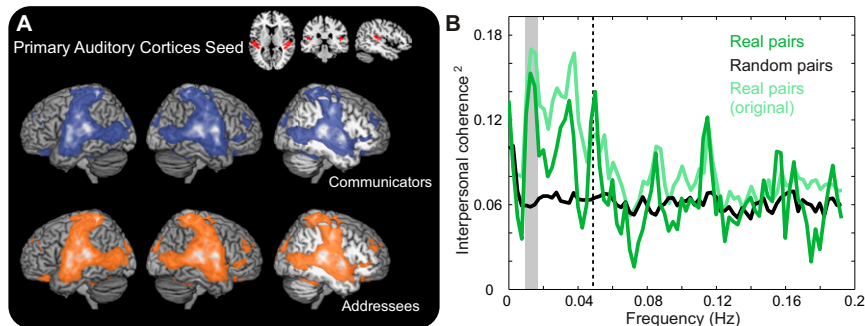


Fig. 56. Control analysis 1. Coherence analysis on rSTG BOLD signal time series after removal of cortical signal related to auditory stimulation found that pair-specific low-frequency interpersonal coherence remained statistically significant (with maximum coherence at 0.0125 Hz; $P = 0.016$). Activity related to auditory stimulation-related activity was indexed with BOLD signal extracted from the primary auditory cortices (ref. 1; Brodmann area 41). The primary auditory cortices were individually defined for each participant on the basis of the spatial overlap between the Brodmann area 41 AFNI template (2) and the participant's segmented gray matter. (A) Spatial distribution of BOLD activity correlated with the primary auditory cortex seed (indicated in red in *Top Right*), separately for Communicators (in blue) and Addressees (in orange). The statistical maps are thresholded at $P < 0.05$, whole-brain FWE corrected. (B) The coherence values obtained in this new analysis are shown in dark green (for real pairs) and in black (for random pairs). The coherence values reported in Fig. 2 for real pairs are shown in light green, for comparison.

- Bandettini PA, Jesmanowicz A, Van Kylen J, Birn RM, Hyde JS (1998) Functional MRI of brain activation induced by scanner acoustic noise. *Magn Reson Med* 39(3):410–416.
- Morosan P, et al. (2001) Human primary auditory cortex: Cytoarchitectonic subdivisions and mapping into a spatial reference system. *Neuroimage* 13(4):684–701.

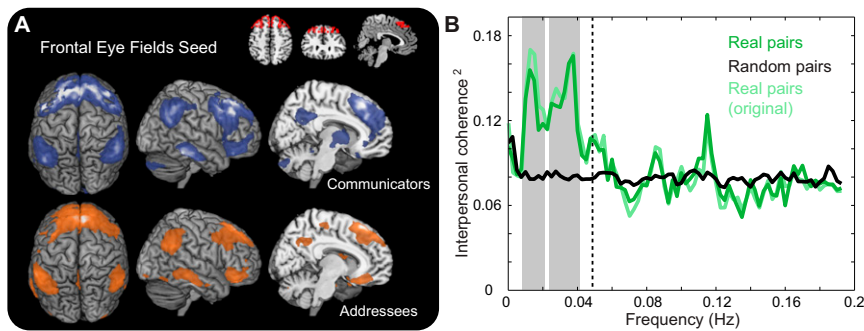


Fig. 57. Control analysis 2. Coherence analysis on rSTG BOLD signal time series after removal of cortical signal related to eye movement found that pair-specific low-frequency interpersonal coherence remained statistically significant (with maximum coherence at 0.0375 Hz; $P = 0.002$). Activity related to eye movement was indexed with BOLD signal extracted from the frontal eye fields (ref. 1; Brodmann area 8). The frontal eyes fields were individually defined for each participant on the basis of the spatial overlap between the Brodmann area 8 AFNI template and the participant's segmented gray matter. (A) Spatial distribution of BOLD activity correlated with the frontal eye field seed (indicated in red in *Top Right*), separately for Communicators (in blue) and Addressees (in orange). The statistical maps are thresholded at $P < 0.05$, whole-brain FWE corrected. (B) The coherence values obtained in this new analysis are shown in dark green (for real pairs) and in black (for random pairs). The coherence values reported in Fig. 2 for real pairs are shown in light green, for comparison.

1. Cheng K, Fujita H, Kanno I, Miura S, Tanaka K (1995) Human cortical regions activated by wide-field visual motion: An H2(15)O PET study. *J Neurophysiol* 74(1):413–427.

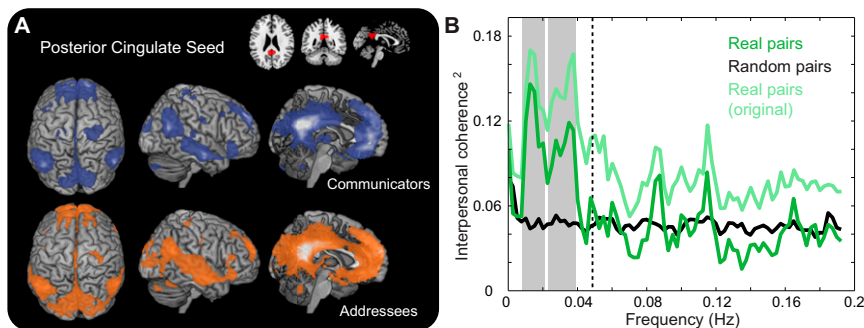


Fig. 58. Control analysis 3. Coherence analysis on rSTG BOLD signal time series after removal of cortical signal related to default-mode activity found that pair-specific low-frequency interpersonal coherence remained statistically significant (with maximum coherence at 0.0125 Hz; $P = 0.004$). Default-mode activity was indexed with BOLD signal extracted from the posterior cingulate cortex (ref. 1; PCC). The posterior cingulate was individually defined for each participant on the basis of the spatial overlap between the PCC AAL template (2) and the participant's segmented gray matter. (A) Spatial distribution of BOLD activity correlated with the PCC seed (indicated in red in *Top Right*), separately for Communicators (in blue) and Addressees (in orange). The statistical maps are thresholded at $P < 0.05$, whole-brain FWE corrected. (B) The coherence values obtained in this new analysis are shown in dark green (for real pairs) and in black (for random pairs). The coherence values reported in Fig. 2 for real pairs are shown in light green, for comparison.

1. Raichle ME, et al. (2001) A default mode of brain function. *Proc Natl Acad Sci USA* 98(2):676–682.

2. Tzourio-Mazoyer N, et al. (2002) Automated anatomical labeling of activations in SPM using a macroscopic anatomical parcellation of the MNI MRI single-subject brain. *Neuroimage* 15(1):273–289.

Table S1. Results of the random effects analyses related to the main effect of problem type (Known vs. Novel; Novel vs. Known) and to the main effect of time (in Novel trials) for Communicators (during production of communicative signals) and for Addressees (during comprehension of those signals)

Effect	Anatomical location	Cluster size	MNI coordinates			t value
			x	y	z	
Communicator						
Known > Novel (Fig. S3)	Right precentral gyrus/insula lobe	33,957	4	-20	23	6.7
	Posterior cingulate cortex	3,134	-3	-53	19	5.5
	Mid orbital gyrus	2,466	-1	55	13	4.6
	Left middle temporal gyrus	1,697	-48	-65	9	4.5
	Right middle temporal gyrus	1,612	48	-65	3	5.0
Novel > Known (Fig. S3)	Left anterior cingulate cortex/inferior frontal gyrus	23,315	-24	18	17	9.1
	Left supramarginal gyrus	17,703	4	-57	39	8.2
	Right middle frontal gyrus	4,794	35	21	34	7.0
	Right inferior frontal gyrus	1,977	51	15	10	6.2
	Right cerebellum	924	21	-75	-30	4.9
Novel _{time} > 0* (Fig. 1C)	Left middle temporal gyrus	5,003	-50	-20	12	7.6
	Right superior temporal gyrus	4,395	53	-14	12	7.1
	Mid orbital gyrus	693	-4	52	-1	5.0
Addressee						
Known > Novel (Fig. S3)	Posterior cingulate cortex	27,949	-15	-34	25	9.0
	Mid orbital gyrus	8,073	-3	46	6	9.0
	Right superior temporal gyrus/insula lobe	7,496	43	-12	2	6.2
	Right middle temporal gyrus	2,263	46	-59	17	5.9
	Left middle temporal gyrus	1,583	-45	-62	26	7.4
Novel > Known (Fig. S3)	Left pallidum/inferior frontal gyrus	28,974	-22	16	17	10.3
	Right inferior frontal gyrus	12,747	34	21	-5	7.9
	Left supramarginal gyrus	6,920	-40	-54	39	7.7
	Right supramarginal gyrus	5,906	40	-53	44	6.1
	Left cerebellum	3,529	-20	-77	-21	5.6
	Right cerebellum	2,311	21	-72	-27	7.8
	Left middle temporal gyrus	1,513	-56	-51	-3	5.6
	Left precuneus	617	-7	-68	47	4.9
Novel _{time} > 0* (Fig. 1C)	Right superior temporal gyrus/insula lobe	1,560	50	-13	11	5.6
	Right precuneus	970	11	-57	18	6.3
	Left superior temporal gyrus	504	-56	-10	5	6.2
Conjunction						
Known > Novel (Fig. S3)	Right superior temporal gyrus/insula lobe	5,159	44	-12	3	5.7
	Left superior temporal gyrus	4,987	-44	-18	1	5.2
	Posterior cingulate cortex	2,461	0	-53	26	5.5
	Middle cingulate cortex	2,327	7	-21	54	4.9
	Left postcentral gyrus	2,205	-34	-24	51	4.2
	Mid orbital gyrus	2,064	-1	55	12	4.4
	Right middle temporal gyrus	566	47	-64	7	3.7
Novel > Known (Fig. S3)	Left inferior frontal gyrus	14,297	-33	22	22	8.4
	Left supramarginal gyrus	4,507	-42	-54	39	7.8
	Right supramarginal gyrus	4,235	41	-55	42	5.8
	Right middle frontal gyrus	3,215	37	21	33	5.8
	Right inferior frontal gyrus	1,782	52	16	11	5.8
	Left putamen	1,395	-11	3	-1	7.1
	Right caudate nucleus	1,236	11	4	-2	5.8
	Right cerebellum	704	20	-74	-30	4.9
Novel _{time} > 0† (Fig. 1C)	Right superior temporal gyrus	829	58	-8	5	4.4

*Masked by the contrasts Known > Novel and Novel_{time} > Known_{time}. Unmasked main effects of time are shown in Fig. S4.

†Masked by the contrasts Known > Novel and Novel_{time} > Known_{time} (in Communicators) and by the contrast Known > Novel (in Addressees).

